HYDROLOGICAL PROCESSES
Hydrol. Process. **21**, 2100–2111 (2007)
Published online 1 May 2007 in Wiley InterScience
(www.interscience.wiley.com) DOI: 10.1002/hyp.6373

Improvement of the hydrological component of an urban soil–vegetation–atmosphere–transfer model

A. Lemonsu,[1]* V. Masson[1] and E. Berthier[2]

[1] *Météo-France, Centre National de Recherches Météorologiques, 42 avenue Coriolis, 31057 Toulouse Cedex, France*
[2] *DREIF-Laboratoire de l'Ouest Parisien, Division Eau-Environnement, 12 rue Teisserenc de Bort, 78190 Trappes, France*

Abstract:

A numerical study was conducted on the Rezé suburban catchment (Nantes, France) to evaluate the hydrological component of the town energy balance (TEB) scheme, which simulates in a coupled way the water and energy balances for the urban covers. The catchment is a residential area where hydrological data were continuously collected from 1993 to 1998 by the Laboratoire Central des Ponts et Chaussées (LCPC), notably the runoff in the stormwater drainage network. A 6-year simulation with the TEB and interaction soil–biosphere–atmosphere (ISBA) schemes in off-line mode enabled the comparison of modelled and observed runoff. Some weaknesses of the TEB were uncovered and led to improved parameterization of water exchanges: (1) calibration of the maximum capacity of the rainfall interception reservoir on roads and roofs and (2) inclusion of water infiltration through the roads, according to a simple formulation. The calibration of this water flux gives results that are consistent with direct measurements of water infiltration performed on the Rezé site and from the literature. The new parameterization produces better runoff in terms of timing and magnitude, which are comparable to those obtained by the LCPC with other hydrological models. It shows also the impact of the water infiltration through the roads, corresponding to a water transfer from the TEB to ISBA, on the water balance: the water contents of road, roof and soil reservoirs being modified, the evaporation from artificial surfaces decreases, while the evapotranspiration from natural covers increases. Through the evaporative flux, such a modification of the water balance induces large repercussions on the surface energy balance. Copyright © 2007 John Wiley & Sons, Ltd.

KEY WORDS urban hydrology; SVAT; urban physically based model

Received 19 September 2005; Accepted 22 May 2006

INTRODUCTION

The water balance is largely modified in the urban environment due to human intervention (Oke, 1987). The same hydrological processes that occur in natural areas are disturbed. The origins of these perturbations are the urban geometry (pattern of roads and roofs), the properties of artificial materials, and the drainage network design. The major characteristics of the urban surface water exchanges are a reduced water storage on built-up covers coupled with a reduced evaporation (Oke, 1982) and a greater surface runoff than from natural surfaces (Boyd *et al*., 1994). Urban surface runoff that reaches the drainage network is the most important water source for the total runoff observed at the outlet of the network. It should be noted that, in certain residential districts, the outdoor water usage for garden watering can represent an important water source and has a significant impact on the evapotranspiration (Grimmond and Oke, 1999a). In the urban soil, the water exchanges are much more complex due to the large heterogeneities in the ground arrangement. Although some experimental studies allowed a better knowledge of the hydrological behaviour and the water balance specific to the urban areas, the different processes are difficult to quantify: urban surface runoff (Hollis and Ovenden, 1988a; Boyd *et al*., 1994; Ragab *et al*., 2003a), water infiltration through the roads (Hollis and Ovenden, 1988b; Ragab *et al*., 2003b), water storage on artificial surfaces (Boyd *et al*., 1993), ground-water infiltration into the sewer network (Belhadj *et al*., 1995).

Modelling studies tried to parameterize these complex mechanisms: Boyd *et al*. (1994) for the runoff, Hollis and Ovenden (1988b) for the depression storage, and Dupasquier *et al*. (1998) for the ground-water infiltration into the sewer network. The recent urban parameterizations used in soil–vegetation–atmosphere–transfer (SVAT) models describe the energy exchanges between the urban surfaces and the atmosphere in a realistic way. But the hydrological component is often non-existent or very simple. When the water exchanges are taken into account, both energy and water balances are resolved and interact through the evaporative term, as in the Grimmond *et al*. (1986) model and in the town energy balance (TEB; Masson, 2000) scheme.

The water balance for a catchment, composed of natural and built-up surfaces, can be written thus:

$$P + I = E + R + D + \Delta W \qquad [\text{kg m}^{-2}\ \text{s}^{-1}] \qquad (1)$$

where P is rainfall, I is the external pipe-water supply (i.e. irrigation and garden watering), E is evaporation,

* Correspondence to: A. Lemonsu, Météo France, Centre National de Recherches Météorologiques, 42 avenue Coriolis, 31057 Toulouse Cedex, France. E-mail: aude.lemonsu@meteo.fr

R is the total runoff in the drainage network, D is the drainage at the bottom and lateral boundaries of the catchment, and ΔW is the variation of water stored at the surface and in the soil during the period of study. Note that here the water balance inside houses (internal water supply and wastewater) is not considered. According to Oke (1987), the urban canopy energy balance is

$$Q^* + Q_F = Q_H + Q_E + \Delta Q_S + \Delta Q_A \quad [\mathrm{W\ m^{-2}}] \quad (2)$$

Q^* is the net all-wave radiation, Q_F is the anthropogenic heat flux, Q_H is the sensible heat flux, Q_E is the latent heat flux, ΔQ_S is the storage heat flux and ΔQ_A the net advective heat flux. The latent heat flux is directly connected to the evaporation E following $Q_E = E/L_v$ with L_v the latent heat of vaporization. As a consequence, water and energy balances are coupled. Hence, modifications of the water balance modify the energy balance and vice versa. This also means that evaporation depends on available water and energy.

This study focuses on the performance of the TEB scheme on an instrumented suburban catchment. In residential areas with gardens, the TEB has to be run with interaction soil–biosphere–atmosphere (ISBA; Noilhan and Planton, 1989), which parameterizes the exchanges between the natural covers and the atmosphere. Both schemes are run in off-line mode, i.e. forced by meteorological observations at a given atmospheric level without being coupled to an atmospheric model. This study aims to:

1. evaluate the water balance resolved by the system TEB–ISBA using a 6-year off-line simulation;
2. improve the water balance calculated by TEB over built-up covers;
3. investigate the impact of the TEB water balance on global water and energy balances.

P and I are input data to TEB–ISBA, and the other terms of the water balance (expressed in Equation (1)) are prognostic variables of the models. Experimentally, the rainfall rate and the runoff at the outlet are recorded at the catchment. For the energy exchanges, Q_F is a TEB input parameter and Q^* is calculated using the observed incident long- and short-wave radiation. The other components of Equation (2) are calculated, except ΔQ_A. The latter is usually assumed to be very small according to the feature of the experimental area and the wind conditions and, consequently, can be neglected.

The following section presents details of the experimental catchment. The third section briefly describes the numerical models. A reference simulation, which is compared with runoff observations (fourth section), identifies the weakness related to the lack of some physical processes, more specifically the water infiltration through the roads. These processes are implemented and the new modelled runoff is investigated in the fifth section. The different terms of the water balance and the sensitivity of the surface energy balance to the changes of the TEB hydrological component are then discussed in the sixth section.

DESCRIPTION OF THE CATCHMENT AND THE DATABASE

The experimental site is the Rezé suburban area, located close to Nantes on the French Atlantic coast (47·20 °N, 1·58 °W). It has an oceanic climate, with moderate annual rainfall (about 800 mm year^{-1}), consisting of a succession of numerous small rainfall events that mainly occur in autumn and winter. The study catchment is a small, 20-year-old residential area of 4·7 ha with single-storied houses and individual gardens (see Figure 1), with short grass and trees. Its drainage network is separated in two networks of pipes: the sewer system that collects the wastewater (domestic and industrial uses) and the stormwater system that collects the water from precipitation (rain or melted snow). The site has been described in detail in Berthier *et al.* (1999). Site information available includes: slope of the site, texture of the soil (clay and sand fractions), road, roof and natural cover fractions, proportion of pervious and impervious surfaces, built-up surfaces connected to the stormwater network, and the spatial distribution of sewer and stormwater networks, which are respectively 803 m and 480 m in length. The subsurface runoff from the ground (under the surface)

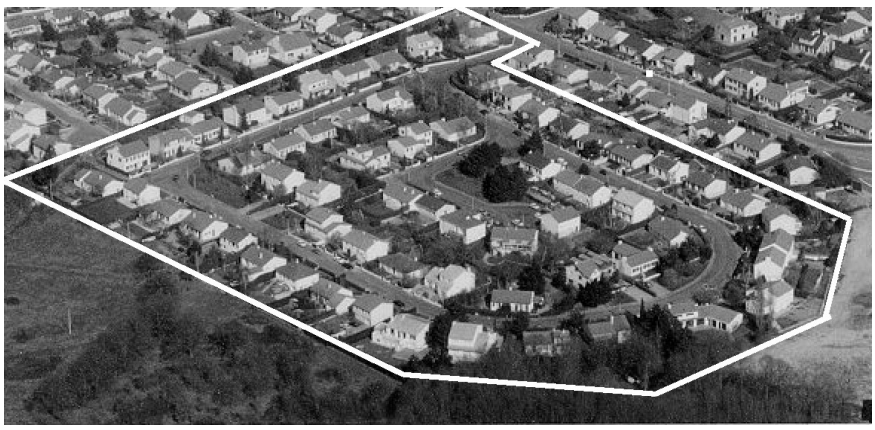

Figure 1. The Rezé suburban catchment (after Berthier *et al.* (2004))

DOI: 10.1002/hyp

is assumed to infiltrate into both networks in proportion to their lengths, i.e. 63% into the sewer network and 37% into the stormwater network. As mentioned previously, the total runoff in the sewer network (wastewater plus infiltrated water) will not be analysed in this paper. However, such a partition seems reasonable compared with observed data (Berthier *et al*., 2004). Of the built-up surfaces, 80% of the roads and 92% of the roofs are connected to the network. The site was instrumented in 1991 by the Laboratoire Central des Ponts et Chaussées (LCPC) and hydrological measurements were collected continuously between 1993 and 1998 (Berthier *et al*., 1999). The rainfall intensity was recorded at three rain gauges. The runoff was measured at the outlet every 1 min. Water table level measurements were also conducted. Data on piped water supply for irrigation were not available. However, contrary to North American suburban areas, where this term is often important (e.g. Grimmond and Oke, 1999a), it is relatively small in the region under study, because of climatic, cultural, and economic reasons. Therefore, external water supply I is assumed to be negligible for this site. The Météo-France operational weather station at Nantes airport, 5 km west of the catchment, provides atmospheric data, i.e. 2 m air temperature and air humidity, 10 m wind velocity, incoming solar radiation, and cloudiness.

Past analyses performed for this catchment include: (1) modelling with the LCPC's physically based urban hydrological element (UHE) model (Berthier *et al*., 2004), which uses a simple parameterization of runoff from impervious surfaces but detailed water transfers within the soil; (2) modelling with URBAN and semi-urbanized runoff flow (SURF) models (Rodriguez *et al*., 2000), more traditional hydrological models, which have been statistically calibrated for this catchment. However, none of these models simulates both energy and water balances, as is done in the SVAT system TEB–ISBA.

BRIEF DESCRIPTION OF THE TOWN ENERGY BALANCE AND INTERACTION SOIL–BIOSPHERE–ATMOSPHERE SCHEMES

The ISBA land-surface scheme is used for exchanges above natural soils and vegetation, whereas the TEB scheme is specifically dedicated to the built-up surfaces.

The ISBA model (Noilhan and Planton, 1989) uses the force–restore method (Deardorff, 1977) and is described in detail in Noilhan and Mahfouf (1996). The subsurface water storage consists of three layers (Boone *et al*., 1999): surface layer, root layer, and deep layer (see Figure 2a). The water sources for the system are rainfall P and dewfall (as noted previously, there is assumed to be no external water use, e.g. irrigation of gardens). The mechanisms of water exchanges are ground evaporation E_g, vegetation evapotranspiration E_v, runoff from root and deep layers (R_2 and R_3 respectively), diffusion between the layers (D_1 and D_2 respectively), and gravitational drainage from the root and the deep layers (K_2 and K_3 respectively). The runoff produced by the deep layer occurs when the water content exceeds the volumetric water content at saturation. In the root layer, it takes place when just one part of the layer is saturated (Habets *et al*., 1999), following Dumenil and Todini (1992).

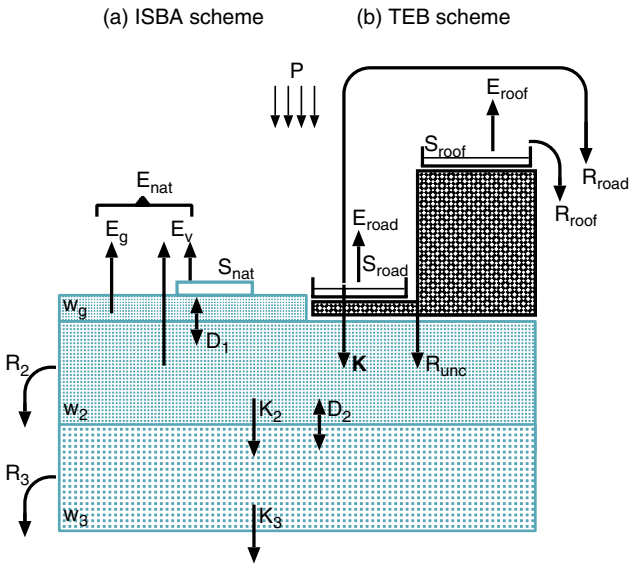

Figure 2. Description of the TEB and ISBA schemes. (a) ISBA: w_g, w_2 and w_3 are the humidity contents of the surface, root and deep layers respectively. S is the water storage by leav surfaces. (b) TEB: S_i represents the water storage by roads and roofs and R_{unc} is the water runoff from artificial surfaces unconnected to the stormwater network. To improve the standard version of TEB–ISBA, the water infiltration through the roads is parameterized as a water flux K (kg m^{-2} s^{-1})

The TEB scheme (Masson, 2000) is based on the three-dimensional geometry of the urban canopy. The urban areas are represented as an ensemble of urban canyons (Oke, 1987) oriented in all directions. Three kinds of surfaces are identified: roads, roofs, and walls. Given the fact that the various types of urban surfaces have specific behaviours, the energy and the water balances are resolved independently for roads, roofs, and walls. For each urban facet, the energy balance accounts for the specific urban material properties, and the energetic and radiative processes (radiation trapping and shadow effects inside the streets). The turbulent exchanges are computed using an aerodynamic resistance network which exchange coefficients depend on the wind speed and the stability conditions. This component of the model has already been studied and evaluated for different areas under dry conditions: an industrial district in Vancouver (BC, Canada) and the dense city core of Mexico City (Mexico) (Masson *et al*., 2002) and Marseille (France) city centre during the ESCOMPTE field campaign (Lemonsu *et al*., 2004). The parameterization of the water exchanges in the TEB is very simple and is based on two assumptions: (1) only the roads and the roofs can intercept water; (2) the built-up surfaces are totally impervious. The source of water for the system is rainfall and dewfall, whereas the losses are evaporation and runoff processes. The principle is described in Figure 2b. Each road and each roof has its own water reservoir. Its water content

DOI: 10.1002/hyp

w_i is computed at every time step following

$$\frac{\partial \omega_i}{\partial t} = P_i - E_i - R_i \qquad [\text{kg m}^{-2}\ \text{s}^{-1}] \qquad (3)$$

where P is the rainfall intercepted by the surface, E is the evaporation, and R is the surface runoff. Note that i stands for roof or road. In the standard version of the TEB, the maximum interception capacity of both road and roof water reservoirs is fixed at 1·0 kg m^{-2}. These terms correspond to the initial losses, i.e. the runoff term is zero unless the computed water content exceeds the maximum interception capacity. In this case, the excess of water leaves the system as a surface runoff. E is computed using the latent heat flux, which is calculated in accordance with the other parts of the energy balance. It depends on surface state (water reservoir, but also temperature) and on atmospheric characteristics (wind, temperature, humidity, stability). Details are given in Masson (2000).

Finally, it should be noted that the ISBA and TEB schemes are run independently for vegetated and built-up areas respectively. Then, both water and energy balances are averaged according to the respective fractions of vegetated and built-up covers. In the initial version of the TEB water balance parameterization, subsoil was not considered under the built-up surfaces and all of the water exchanges took place at the surface. In the present study, since the TEB does not include a soil reservoir, the root zone and deep soil layers of ISBA are extended below the built-up surfaces (see Figure 2), which assumes horizontal homogeneity of water content within the soil. At the scale of a property, this is a reasonable approximation, both because of the small horizontal scale and the nature of the disturbed soil properties. A simple interaction between ISBA and TEB is also parameterized: the surface runoff from road and roof fractions unconnected to the stormwater network is injected into the ISBA root-zone water reservoir (R_{unc} in Figure 2).

Table I. Parameters of the ISBA and TEB schemes

General parameters	
Garden fraction	0·555
Town fraction	0·445
TEB parameters	
Total roof fraction	0·168
Total road fraction	0·277
Canyon aspect ratio h/w	0·37
Ratio of wall surface to roof and road surface	0·76
House height (m)	5·9
Roughness length for momentum (m)	0·59
Main roof material	Tile
Main road material	Asphalt
Main wall material	Concrete
ISBA parameters	
Root layer thickness (m)	1·00
Deep layer thickness (m)	1·00
Slope of the soil water retention curve	0·1
Vegetation fraction in gardens	0·95
Bare soil fraction in gardens	0·05
Vegetation leaf area index	1–3
Vegetation albedo	0·2
Vegetation roughness length for momentum (m)	0·01
Initial water contents (January 1993)	
Surface and root layers	Field capacity
Deep layer	Saturated

DESCRIPTION OF THE SIMULATION

Forcing data and input parameters

A 6-year simulation of the suburban catchment is performed using the ISBA and TEB schemes in off-line mode on one single grid point, from 1 January 1993 to 31 December 1998. The forcing data are air temperature, specific humidity, wind direction and wind speed, surface pressure, rainfall, and incoming short- and long-wave radiation. Most of them come from the observations of the Météo France station (see the 'Description of the catchment and the database' section), whereas the rainfall rate is defined by the measurements collected at the site. In addition, the incoming longwave radiation was computed using the Prata (1996) formulation, which takes cloudiness into account. These input data force the model every 30 min, except for the rainfall, which is applied with the same frequency as the model time-step, i.e. 5 min. Note that there were no snow events during the period.

All the TEB descriptive parameters are presented in Table I. Some of the morphological data of the urban covers were already documented by the LCPC, like roof and road fractions and the mean height of the houses of about 5·9 m. The roughness length for momentum was estimated to be 0·59 m for this suburban site, equal to one-tenth of the house height (Grimmond and Oke, 1999b). The other parameters and the radiative and thermal properties of materials are defined from analysis of aerial photographs and from the literature (Oke, 1982; Mills, 1993). Since the catchment is a purely residential suburban area, anthropogenic fluxes due to traffic and industrial activities are neglected. However, the impact of domestic heating is implicitly taken into account, given the fact that the TEB lays down a minimum internal building temperature, which may produce heat release during wintertime. The ISBA input parameters characterize the soil and vegetation properties (Table I). Considering the description of the catchment, they are defined as averaged parameters representative of vegetated covers composed of short grass and trees. The leaf area index (LAI) varies from 1 m^2 m^{-2} in winter to 3 m^2 m^{-2} in summer.

At the experimental site, the water table depth was observed to vary between 0·5 and 1·8 m from the surface. The drainage term D (Equation (1)) is generally a flux of water from the deep layer towards the water table. By using in ISBA a soil layer of about 2 m depth, the top of the water table is always included in the simulation domain. Therefore, the gravitational drainage D takes place within the soil model itself and is then assumed to be negligible at the bottom of the ISBA third layer.

DOI: 10.1002/hyp

The evolution of the water table level is not computed explicitly in the model, but is simply estimated by the accumulation or removal of water in the deep reservoir (by drainage from the root zone or by diffusion). In particular, the deep layer should be saturated in winter, as it would be entirely contained inside the water table.

Results of the reference simulation

A first reference simulation (labelled SREF) is conducted with the initial version and the standard configuration of the TEB and ISBA. The maximum interception capacity of both roofs and roads is fixed at 1·0 kg m^{-2}. The runoff outputs are equal to the sum of all the runoff terms produced by vegetated (ISBA scheme) and built-up (TEB scheme) areas. These water volumes are not directly comparable to the runoff observations because the modelled runoff corresponds to the total water quantity that leaves the system, whereas the measurements refer to the water quantity collected by the stormwater drainage network. It should be noted that, owing to the lack of measurements of wastewater and drinking water volumes, the present study focuses on the evaluation of the stormwater balance. The eventual interaction with the drinking and wastewater balances is taking into account as follows: (1) the drinking water volume received by the ground is assumed to be negligible because garden watering is very limited at the Rezé site; (2) water exfiltration from the sewer network to the ground is negligible; (3) water from the ground infiltrates into the sewer and the stormwater networks in proportion to their length (as mentioned in Section 2), i.e. 63% and 37%, respectively. Besides, the roads and roofs are not entirely connected to the network ('Description of the catchment and the database' section). As a result, the total modelled runoff R_{tot} reaching the stormwater network outlet is

$$R_{\text{tot}} = a_{\text{nat}} a_{\text{inf}} (R_{\text{lay2}} + R_{\text{lay3}}) + f_{\text{roof}} a_{\text{roof}} R_{\text{roof}} + f_{\text{road}} a_{\text{road}} R_{\text{road}} \ [\text{kg m}^{-2}\ \text{s}^{-1}] \quad (4)$$

R_{lay2} and R_{lay3} are the runoffs from the ISBA hydrological layers (see Figure 2a); R_{road} and R_{roof} are the TEB runoffs from roads and roofs (see Figure 2b); a_{nat} is the total fraction of natural covers (i.e. the total pervious area); a_{road} and a_{roof} are the total fractions of roads and roofs, $a_{\text{road}} + a_{\text{roof}}$ being the total impervious area; a_{inf} is the fraction of soil water infiltrated in the drainage networks that reaches the stormwater network (37%); $f_{\text{road}} a_{\text{road}}$ and $f_{\text{road}} a_{\text{road}}$ correspond to the effective impervious areas, with f_{road} and f_{roof} the road and roof fractions connected with the stormwater network (80% and 92% respectively). The runoff is computed every 5 min. The total modelled runoff is transferred to the outlet of the catchment, where the measurements are conducted with a transfer function following Rodriguez *et al.* (2000). Owing to the size of the catchment, all of the runoff reaches the outlet in less than 20 min.

The experimental set-up to measure the runoff is efficient for a non-negligible water quantity. The runoff measurements at the outlet are satisfactory only during rainfall events (Berthier *et al.*, 1999). Therefore, in the present study, although the simulation is performed continuously for 6 years and the runoff outputs are also available continuously, the statistical scores for the modelled runoff are only computed for the rainfall periods. Berthier *et al.* (2004) identified 859 rainfall events, between 1993 and 1998, that lasted at least 1 h with an intensity exceeding 0·5 mm h^{-1}. The Nash criterion C_{Nash} (Nash and Sutcliffe, 1970) and the mean relative error E_{rel} are computed by using the 5-min runoff averaged with a 1 h time-step:

$$C_{\text{Nash}} = 1 - \frac{\sum_n (R_{\text{obs}_n} - R_{\text{sim}_n})^2}{\sum_n (R_{\text{obs}_n} R_{\text{obs}_{\text{avg}}})^2} \quad (5)$$

$$E_{\text{rel}} = \frac{\sum_n (R_{\text{sim}_n} - R_{\text{obs}_n})}{\sum_n R_{\text{obs}_n}} \times 100 \quad [\%] \quad (6)$$

R_{obs_n} and R_{sim_n} are the 1 h average observed and modelled runoffs respectively, and $R_{\text{obs}_{\text{avg}}}$ is the averaged observed runoff. C_{Nash} characterizes the quality of restitution of the runoff variability (i.e. timing and magnitude of peaks). $C_{\text{Nash}} \leq 1$. The better the simulation is, the closer C_{Nash} is to unity. E_{rel} quantifies the errors in terms of runoff magnitude.

In SREF, the statistical results computed for the rainfall events of the period 1993–1998 give E_{rel} equal to about +39% and $C_{\text{Nash}} = 0{\cdot}72$. The runoff is found to be overestimated by the model throughout the 6 years. In addition, the runoff peaks occur too early in comparison with the observations. In conclusion, the built-up surfaces have very low inertia and the response of the surface runoff to the rainfall is too rapid: it appears as soon as cumulative rainfall exceeds 1 mm and returns to zero when there is no more precipitation. Since the largest part of runoff is produced by the roads and the roofs, the error is probably due to the TEB parameterization of water exchanges for the artificial surfaces.

IMPROVEMENT OF THE TOWN ENERGY BALANCE PARAMETERIZATION

Water infiltration through the roads

According to previous studies that focused on the hydrological behaviour of built-up surfaces, a part of the rainfall intercepted by the artificial surfaces can reach the subsoil. This water transfer corresponds to continuing losses generated by two different mechanisms: (1) direct water infiltration through the pavement constituent material and (2) water infiltration through defects in watertightness of the road, such as cracks and crevices. The magnitude of each of these terms is very poorly understood and appears strongly dependent on the study area. Experimental studies present global

DOI: 10.1002/hyp

values of infiltration, including the two mechanisms described, varying between 10^{-2} and 10^{-6} kg m^{-2} s^{-1} (Hollis and Ovenden, 1988a; Hassan and White, 1997; Ragab *et al*., 2003b; Ramier *et al*., 2004). For the Rezé catchment, measurements of water infiltration through the pavement by an infiltrometer, such as those developed by Cooley *et al*. (2001), were conducted in different locations. The results vary considerably according to the samplings of roads: the water infiltration is negligible at two measurement sites, whereas it is about $(3{\cdot}0–5{\cdot}0) \times 10^{-5}$ kg m^{-2} s^{-1} elsewhere and even reaches $1{\cdot}0 \times 10^{-2}$ kg m^{-2} s^{-1} for the last measurement location.

In numerical models, the process is generally assumed to be a constant water flux k (kg m^{-2} s^{-1}), e.g. in the UHE (Berthier *et al*., 2004) or SM2-U (Dupont, 2001) models. In the present study, the road water-infiltration term is parameterized in the TEB in the same way and is added in the road-reservoir evolution equation:

$$\frac{\partial \omega_{\text{road}}}{\partial t} = R_{\text{road}} - E_{\text{road}} - k\delta_{\text{wet}} \quad [\text{kg m}^{-2}\ \text{s}^{-1}] \qquad (7)$$

where δ_{wet} is the road wet fraction and k is the water infiltration through the roads. The water quantity that leaves the system this way is injected into the ISBA root-zone layer (see Figure 2). As previously shown in experimental studies, and even for the Rezé catchment, high variability is encountered because of the surface materials, the surface condition and the pattern of the streets. Consequently, the value of this flux cannot be directly initialized, but it has to be calibrated for the TEB–ISBA simulation of the Rezé catchment. This was already done for the UHE model (Berthier *et al*., 2004).

Considering the whole system (roads, houses and gardens), the water balance follows Equation (1). For roads and roofs only, it takes the following form:

$$P = E_{\text{built}} + R_{\text{built}} + K + \Delta W_{\text{road}} + \Delta W_{\text{roof}} \quad [\text{kg m}^{-2}\ \text{s}^{-1}] \qquad (8)$$

R_{built} is surface runoff from built-up areas. ΔW_{road} and ΔW_{roof} are the variations in water storage for roads and roofs. K represents the total water infiltration through the roads into the subsurface, which is dependent on the constant flux k and the road wet fraction ($K = k\delta_{\text{wet}}$). The evaporation E_{built} is a very important component of the balance, but is not experimentally documented here. In order to limit the number of unknown terms, the study is focused on the rainfall events, where the evaporation is zero. In this case, the water balance of artificial surfaces is reduced to

$$P = R_{\text{built}} + K + \Delta W_{\text{road}} + \Delta W_{\text{roof}} \quad [\text{kg m}^{-2}\ \text{s}^{-1}] \qquad (9)$$

A correct estimation of K and ΔW_i is necessary to simulate R_{built} successfully. Conversely, R_{built} can be used to validate K and ΔW_i. However, only the total runoff R is observed at the outlet, and it is required to estimate the runoff produced by the built parts.

During the summer on the Rezé catchment, because of small rainfall and large vegetation transpiration, soils are dry (much below saturation) and are not able to produce runoff or infiltration into the stormwater network (Berthier *et al*., 2004). The runoff is only produced by the artificial surfaces and $R = R_{\text{built}}$. As a consequence, in the next section, the calibration of water infiltration and maximum water interception capacities of the TEB is conducted exclusively on the 152 summer rainfall events between 1993 and 1998, in order to avoid influence from natural covers. Afterwards, the evaluation of the whole simulation is done on all of the rainfall events identified during the six complete years used as an evaluation period (see 'Evaluation on all rainfall events' section).

Calibrations on summer rainfall events

Three calibration exercices were performed: (1) maximum water interception capacity calibration without taking the water infiltration into account; (2) calibration of the water infiltration k by keeping the roof and road maximum water interception capacities to the reference values; (3) calibration tests coupling the two mechanisms.

The road and roof materials and the urban design influence the water storage on urban surfaces, and consequently the evaporation, runoff, and infiltration processes. The water-reservoir sizes can vary from 0 to 6·0 kg m^{-2} according to Hollis and Ovenden (1988b), Grimmond and Oke (1991) and Boyd *et al*. (1993). In the present case, this range of values is applied to the road maximum water interception capacity, when the roof maximum water interception capacity is fixed to 0·5 kg m^{-2} as in Berthier *et al*. (2004), because the roof slopes limit the water storage. To increase the water storage capacity on roads delays and limits the road surface runoff and, thus, the global runoff from TEB–ISBA, which leads to an improvement of the modelling results. The best statistical scores (Figure 3a and b) are obtained for the test using the highest road maximum water interception capacity.

According to the literature values and *in situ* observations (see previous section), k is tested between 0 and $1{\cdot}0 \times 10^{-2}$ kg m^{-2} s^{-1}. As previously, the inclusion of the infiltration mechanism tends to limit the road surface runoff because less water is stored on the roads. The statistical scores of the water infiltration calibration (Figure 3c and d) underline two different behaviours. For the lowest values of water infiltration flux, i.e. from 0 to $2{\cdot}0 \times 10^{-4}$ kg m^{-2} s^{-1}, the delay of the road surface runoff induces a delay of the global runoff, which considerably improves the scores. First, the greater the water infiltration is, the closer C_{Nash} is to unity (not shown). Second, since the runoff decreases when the infiltration increases, the magnitude is also modelled better. For the highest values starting from $1{\cdot}0 \times 10^{-3}$ kg m^{-2}, the infiltration process injects more water into the ISBA root-zone layer. For the rainiest summers, this generates a lateral runoff from natural vegetation area that degrades the Nash criterion. The magnitude of the global runoff is considerably underestimated.

DOI: 10.1002/hyp

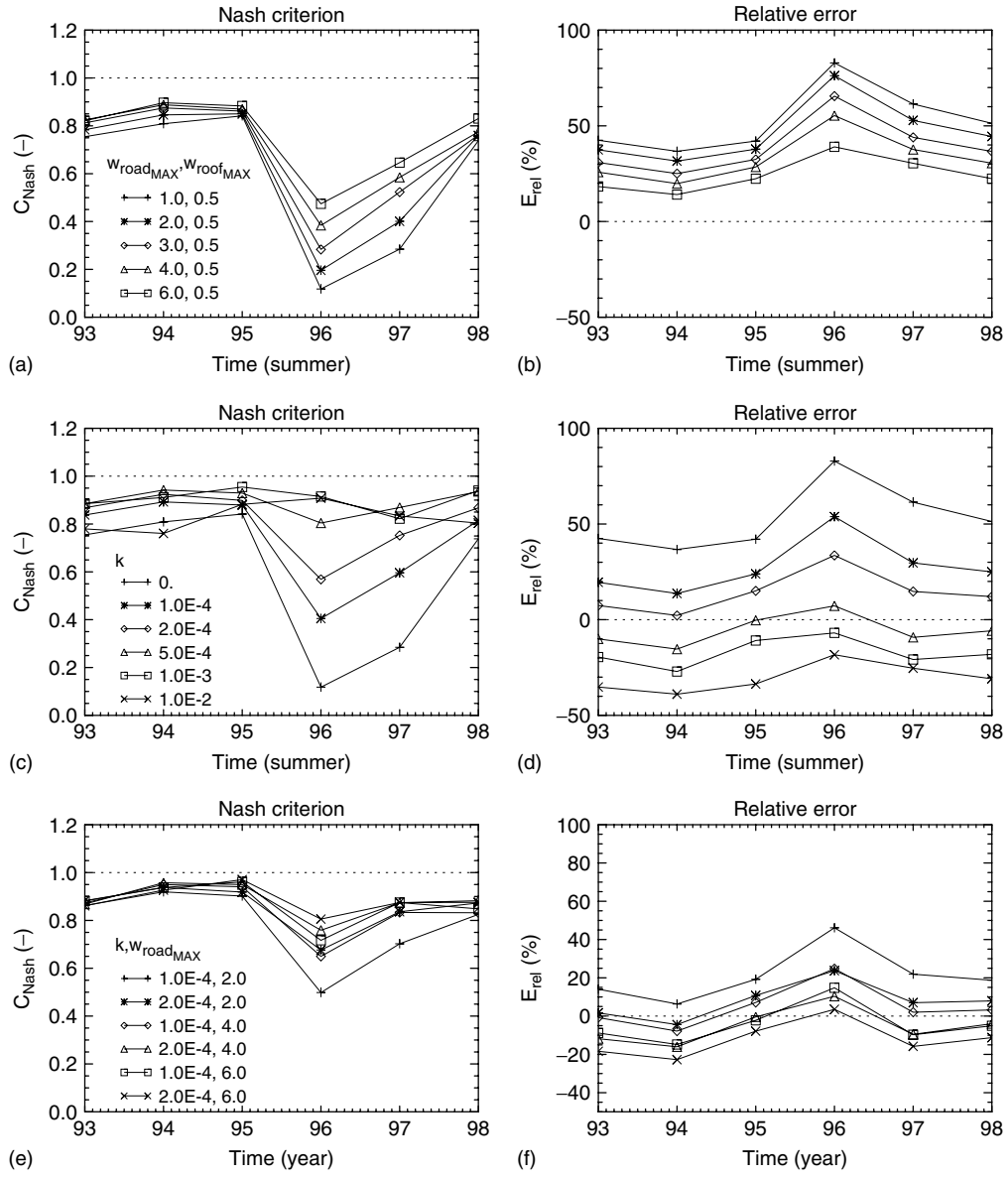

Figure 3. (a) and (b) Calibration of the water infiltration through the roads. k varies between 0 and 1×10^{-2} kg m^{-2} s^{-1}, when the maximum water interception capacities of both roads and roofs are equal to 1 kg m^{-2}. (c) and (d) Calibration of the road maximum water interception capacity. It varies between 1 and 6 kg m^{-2} (or millimetres) when k is assumed to be zero. (e) and (f) Calibration of coupling the water infiltration and the maximum water interception capacities. k varies between 0 and 1×10^{-2} kg m^{-2} s^{-1} and the road maximum water interception capacity varies between 2 and 6 kg m^{-2} when the roof maximum water interception capacity is fixed at 0·5 kg m^{-2}. Hourly Nash criteria (left) and relative errors (right) are computed for all summer rainfall events identified between 1993 and 1998

It should be noted that the inclusion of the water infiltration mechanism has a larger impact on the runoff than the variation of the reservoir's size. However, the efficiency of the water infiltration mechanism is directly dependent on the reservoir's size, which determines the available water volume on the roads. For the last calibration exercise, extensive tests were performed by coupling the two mechanisms for all the values applied in the previous calibration tests. The most interesting results are presented in Figure 3e and f, with water infiltration flux values of $1{\cdot}0 \times 10^{-4}$ and $2{\cdot}0 \times 10^{-4}$ kg m^{-2} s^{-1} and road water interception capacities of 2·0, 4·0 and 6·0 kg m^{-2}. In conclusion of this sensitivity study, the best results are obtained for $w_{\mathrm{roadMAX}} = 4{\cdot}0$ kg m^{-2}, $w_{\mathrm{roofMAX}} = 0{\cdot}5$ kg m^{-2} and $k = 1{\cdot}5 \times 10^{-4}$ kg m^{-2} s^{-1}. Table II shows that the maximum interception capacities are really comparable to those determined in the UHE (Berthier *et al*., 2004), and also to those obtained from the statistical calibration of the hydrological URBAN and SURF models (Rodriguez *et al*., 2000). The water infiltration flux is of the same order of magnitude as the experimental values (see 'Water infiltration through the roads' section), more specifically for the water infiltration that was measured at the Rezé site (between $3{\cdot}0 \times 10^{-5}$ and $1{\cdot}0 \times 10^{-2}$ kg m^{-2} s^{-1}).

In the following sections, the paper focuses on the analysis of four of the previously presented tests in order to illustrate the impact of the different mechanisms included in the TEB on the performances of the model: (1) SREF is the reference simulation

DOI: 10.1002/hyp

Table II. Results from calibration of model parameters, for UHE (from Berthier *et al.* (2004)) and TEB models

	UHE	TEB
Infiltration capacity (kg m^{-2} s^{-1})	$7{\cdot}5 \times 10^{-5}$	$1{\cdot}5 \times 10^{-4}$
Maximum road interception capacity (kg m^{-2})	3·5	4·0
Maximum roof interception capacity (kg m^{-2})	0·5	0·5

already described in the 'Description of the simulation' section; (2) SWMAX only takes the calibration results of the maximum interception capacities into account ($w_{\mathrm{roadMAX}} = 4{\cdot}0$ kg m^{-2} and $w_{\mathrm{roofMAX}} = 0{\cdot}5$ kg m^{-2}); (3) SINF includes the water infiltration mechanism ($k = 1{\cdot}5 \times 10^{-4}$ kg m^{-2} s^{-1}) while keeping the standard sizes of road and roof water reservoirs; finally (4) SCPL refers to the coupling of the two calibration results ($w_{\mathrm{roadMAX}} = 4{\cdot}0$ kg m^{-2}, $w_{\mathrm{roofMAX}} = 0{\cdot}5$ kg m^{-2}, and $k = 1{\cdot}5 \times 10^{-4}$ kg m^{-2} s^{-1}). All the characteristics of these simulations are listed in Table III.

Evaluation of all rainfall events

The use of all rainfall events (i.e. summertime rainfall events and all of those not used previously) enables evaluation of the accuracy of the model, because data independent of those used in the calibration process are now considered. During winter, in addition to the runoff from artificial surfaces, the action of the vegetated areas is no longer negligible, due to direct water infiltration from the soil into the stormwater drainage network. Indeed, the observations show that the water table is less than 0·5 m from the surface, which is above the stormwater and sewer networks (which are located at least 1·0 m deep). Runoff is generated into both of these systems. ISBA simulates this runoff, as the deep layer is saturated in winter, as expected. The water transfer from the TEB to ISBA, via the water flux K, and the two subsequent calibrations, improved the timing and the magnitude of the runoff, as seen in the examples for two rainfall events (Figure 4). The annual statistical scores are presented in Figure 5. The TEB reservoir calibration produces slightly better runoffs, but the improvement, both in terms of timing and magnitude, is primarily related to the inclusion of K.

Table IV. Comparison of the statistical scores of the simulations using the different calibration processes. They were computed from the runoff outputs of the 859 rainfall events identified between 1993 and 1998

	Global C_{Nash}	Global E_{rel} (%)
SREF	0·72	+38·6
SWMAX	0·77	+31·3
SINF	0·86	−9·6
SCPL	0·89	−4·1

The global statistical scores computed for SREF, SWMAX, SINF and SCPL (with or without each calibrated process) are given in Table IV. After the two calibrations of water infiltration and water reservoirs, global $C_{\mathrm{Nash}} = 0{\cdot}89$ and global $E_{\mathrm{rel}} = -4{\cdot}1\%$. These are satisfactory results for a physically based model.

DISCUSSION

Water balance

The modified version of TEB–ISBA has been evaluated previously. The present section investigates the global water balance and the impact of all of the components in the different cases. All terms have been normalized by the total rainfall rate on the catchment.

The water balance of SREF is presented in Figure 6. The evaporation from natural areas is the predominant term, i.e. 53·1% of total rainfall precipitated. On built-up areas, the size of the water reservoirs (1·0 kg m^{-2} for both roads and roofs) is too small to produce a comparable flux. Evaporation of intercepted rainfall is only 6·5% from the built-up surfaces, despite the area fractions being very similar (see Table I). However, the largest fraction of the total runoff is observed on the built-up surfaces (32·0% for the TEB against 9·1% for ISBA). This urban runoff comes from roads (19·0%) and roofs (13·0%) based on their relative fractions. As some of the built surfaces are not connected to the stormwater drainage network, 5·9% of the rainfall is injected into the second ISBA hydrological layer.

The calibration of the water interception capacities alone has a limited impact on the global water balance partitioning (SWMAX on Figure 6). Since the roads store more water, it induces a decrease of the road runoff (16·5% instead 19·0%) associated with an increase of the road evaporation (7·0% instead 3·9%). Conversely,

Table III. Description of the different performed simulations

Simulation	Description	w_{roadMAX} (kg m^{-2})	w_{roofMAX} (kg m^{-2})	k (kg m^{-2} s^{-1})
SREF	Standard configuration of the TEB	1·0	1·0	0
SWMAX	Calibration of maximum water interception capacity of roads and roofs	4·0	0·5	0
SINF	Calibration of water infiltration through the roads	1·0	1·0	$1{\cdot}5 \times 10^{-4}$
SCPL	Coupled calibration of maximum water interception capacity of roads and roofs and water infiltration through the roads	4·0	0·5	$1{\cdot}5 \times 10^{-4}$

DOI: 10.1002/hyp

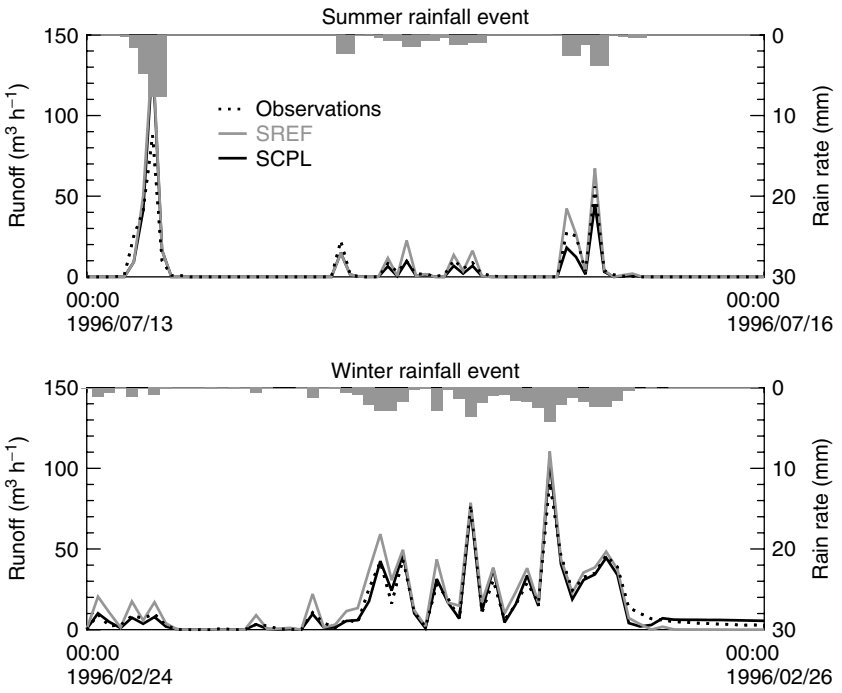

Figure 4. Hourly observed and modelled runoffs during summer and winter rainfall events. SREF and final results of SCPL are compared with the runoff observations

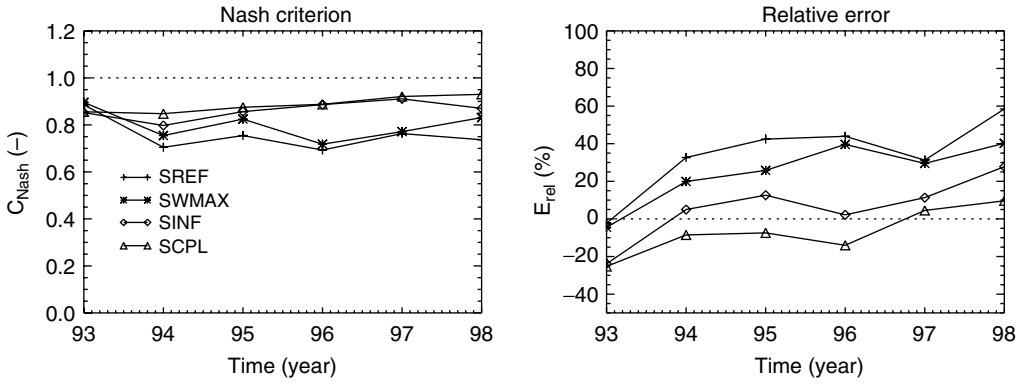

Figure 5. Comparison of the statistical results computed for annual rainfall events for SREF, SWMAX, SINF and SCPL

since the roof interception capacity is only 0·5 kg m^{-2} for SWMAX, the roof runoff is slightly stronger (13·8%) and the roof evaporation is weaker (1·8%) than in SREF.

The inclusion of K induces perturbations at the road scale and at the catchment scale. The road evaporative term becomes weak, the water infiltration mechanism being faster and more efficient than the evaporation process. This represents a supplementary source of water for ISBA, which explains the strong increase of runoff (17·8% in SINF and 21·4% in SCPL, instead of 9·1% in SREF) and the slight increase of evapotranspiration in SCPL (53·3%) from the ground. Note that just one part of the runoff from the ground reaches the stormwater network and, consequently, arrives at the outlet. This term represents 7·9% of the total rainfall in SCPL, which is in agreement with the UHE model results (Berthier *et al*., 2004). The water transfer term (through the roads) represents 19·3% of the total rainfall in the TEB water balance of SCPL, which is high. Some physical processes could play an important role in the water transfer from the road surfaces to the natural surfaces and to the stormwater drainage network. They could explain the large influence of the water infiltration component: (a) the small slope of the area and the age of the roads can favour the formation of water puddles in some parts of the pavement, which are no longer connected to the stormwater drainage network; (b) the light rainfall rates generally encountered under the oceanic climate favour the infiltration process, because the light rains limit the filling of the road water reservoir, thus preventing runoff. Anyway, the lack of knowledge on the physical process and on its magnitude is obvious. Once more, the process appears strongly variable from one stretch of road to another, and even from one point to another of a same road stretch. Our work and the Rezé database do not appear suitable to progress in the knowledge of the road infiltration process. These

DOI: 10.1002/hyp

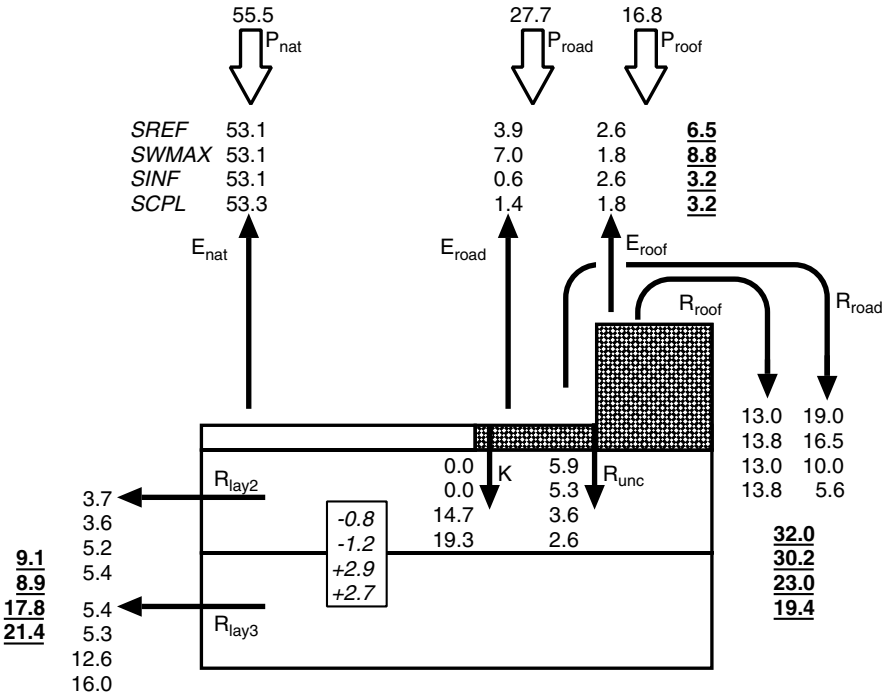

Figure 6. Description of the water balance (units: percentage of the total runoff) obtained by SREF, SINF, SWMAX and SCPL simulations. R_{unc} is the water infiltration into the root layer (due to the runoff from the artificial surfaces unconnected to the network) and K is the water infiltration through the roads. All the terms are computed as a percentage of the total rainfall. The underlined terms are the components of the balance and the non-underlined terms are the separated terms by surface type. The italic terms indicate the variations of the soil water content during the 6-year simulation

considerations do not involve the existence of K in the TEB: an equivalent flux exists *in situ*, and in the model its magnitude allows one to reproduce total runoff correctly at the outlet. The physical interpretation of its hydrological role must only be done with caution, and this is why the k parameter is considered as a calibration parameter.

Surface energy balance

With ISBA and the TEB, being physically based models, the water and energy balances interact through the evaporative term (see 'Introduction'). The present section aims at evaluating how the changes of the TEB hydrological component influence the energy exchanges between the catchment and the atmosphere. This study focuses on the rainy periods when the TEB–ISBA system is much more affected by the new parameterization.

Figure 7 presents the SREF and SCPL surface energy balances averaged on all the rainy days of the integration period. Since the ISBA and TEB schemes are run independently, three different balances are displayed: the ISBA energy balance relative to the vegetated areas, the TEB energy balance relative to built-up areas, and the energy balance of the system TEB–ISBA calculated as the averaged of the first two balances according to the fractions of vegetated and built-up covers.

The ISBA energy balance is not significantly influenced by the modification of the TEB hydrological component, although the water balances presented in the previous section show a small increase in evaporation for vegetated covers (Figure 6). The TEB energy balance is obviously affected by the mechanism of water infiltration through the roads and the calibration of the roof maximum interception capacity. Both limit the evaporation on roads and roofs and, consequently, tend to reduce the turbulent latent heat flux. All the energy not used by the latent heat flux is transferred to the sensible heat flux, whereas the storage heat flux does not change. The weight of each component is calculated for the daytime period (when the net radiation is positive). Thus, daytime Q_E, Q_H and ΔQ_S respectively represent 44%, 38% and 18% of the net radiation for SREF, whereas their contributions are 35%, 46% and 19% respectively for SCPL.

The trends observed on the global energy balance of the TEB–ISBA system are similar to those observed for the TEB. However, the impact on the turbulent fluxes is attenuated, considering that the built-up fraction only covers 45% of the catchment. In this case, the contributions of Q_E, Q_H and ΔQ_S are equal to 54%, 27% and 19% respectively for SREF, and then reach 49%, 31% and 20% respectively for SCPL. In addition, the Bowen ratio (expressed as Q_H/Q_E) increases from 0·50 in SREF to 0·63 in SCPL.

These results indicate that the new parameterization of water exchanges applied for the TEB also influences the production of turbulent fluxes over the built-up covers, but does not seem to affect the energy exchanges over the vegetated covers. As a result, and considering the calculation method for the global TEB–ISBA energy balance, the latter may be more or less influenced according to the fraction of built-up covers. Unfortunately, no energy flux observation is available on the experimental site to

DOI: 10.1002/hyp

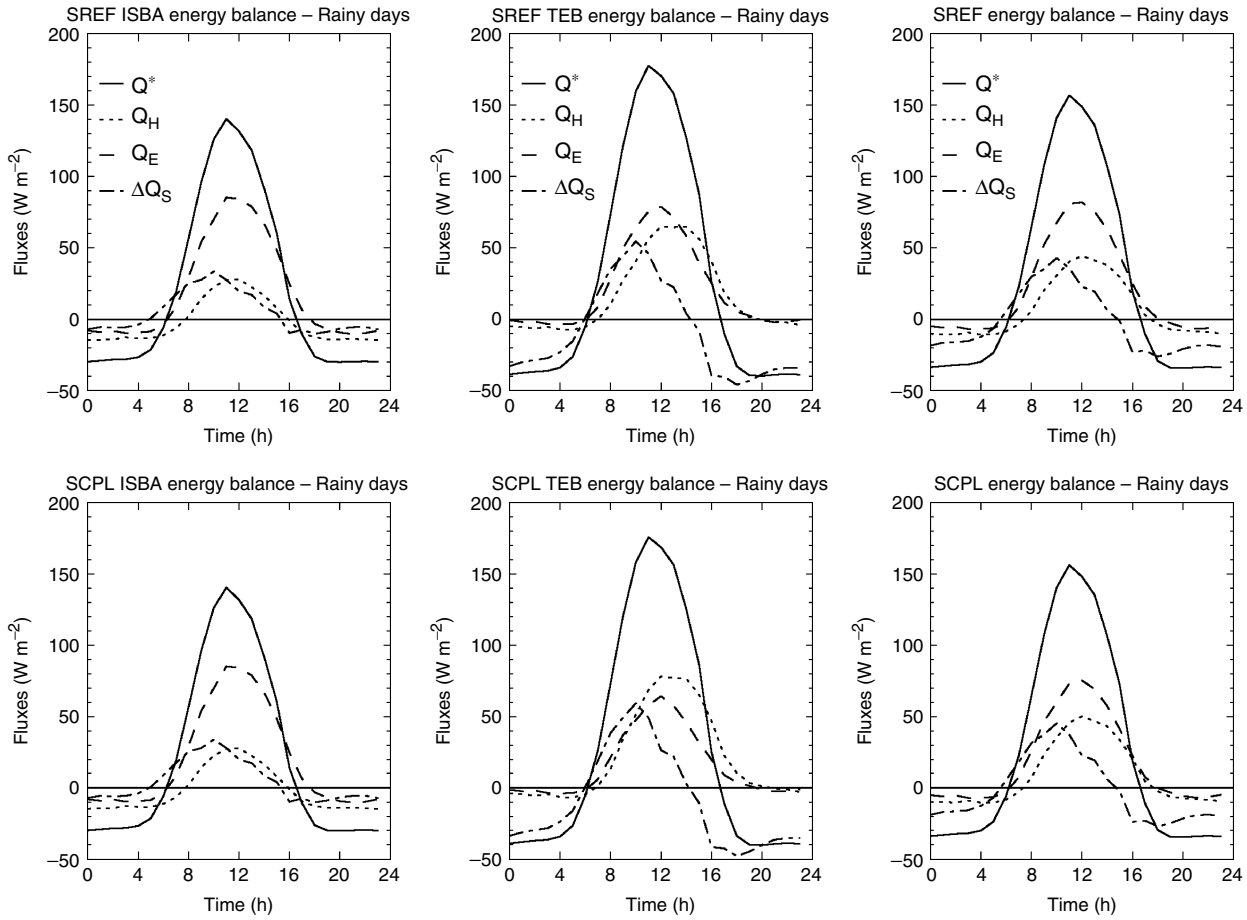

Figure 7. Surface energy balances simulated with SREF (top) and SCPL (bottom) and averaged on the rainy days for ISBA (left), TEB (middle) and TEB–ISBA (right)

quantify the turbulent fluxes and evaluate the model performances.

CONCLUSIONS

This study discusses the parameterization of urban hydrological mechanisms, which were not included in the initial version of the physically based TEB urban canopy model. First, the inclusion of water infiltration through the roads reduces the surface runoff from roads, which improves both magnitude and timing of the total modelled runoff at the outlet. Second, the calibration of road and roof maximum interception capacities leads to a slightly more realistic water storage for these urban surfaces. Thus, the evaluation of the model against observations highlights that the modifications of the TEB hydrological component improve the performances of the TEB–ISBA system to simulate the total runoff. Although both water infiltration and water storage have an impact on the water balance, the water transfer mechanism from the TEB to ISBA is the most significant process. It influences all of the water exchanges for the vegetated and built-up surfaces. In particular, evaporation from the roads is significantly reduced and evapotranspiration from the ground is slightly increased. The surface energy balance is also modified, i.e. the latent heat flux is smaller, which induces an increase of the other components. This aspect of the study underlines the importance of including a realistic parameterization of the water exchanges in the current urban canopy models used in atmospheric modelling. Most of them do not take the hydrological processes into account, which, however, influence the surface energy balance and, thus, the interactions with the atmosphere.

In this study, the characteristics of the Rezé catchment are well known, which makes possible the evaluation of water runoff to the drainage network, of surface runoff to the ground from built surfaces unconnected to the network, of water exchanges from the roads to the soil by the infiltration process, and of depression storage. However, it is difficult to generalize the conclusions to other areas, even if we focused on the relative impact of some unusual processes leading to the transfer of water from the roads into the soil below. Currently, experimental work is being conducted by the LCPC to study these processes directly, more specifically the infiltration through the pavement constituent material (Ramier *et al.*, 2004).

Water and energy exchanges in urbanized environments are particularly difficult to parameterize and to evaluate, considering the human intervention and the complex interactions that take place between vegetated

DOI: 10.1002/hyp

and built-up covers. The urban evapotranspiration, in particular the anthropogenic control of irrigation of the pervious component and the input of water from the impervious to the pervious area via lateral flows, could play an important role in the water cycle. These aspects were not considered here because they require a complete documentation of water and energy fluxes, which was not available. However, they constitute a major subject of investigation for future work.

ACKNOWLEDGEMENTS

We are very grateful to Dr Joël Noilhan of the Centre National de Recherches Météorologiques of Météo-France and Dr Hervé Andrieu of the Laboratoire Central des Ponts et Chaussées for their assistance and their continuous help. This study received financial support from the French Research Program in Hydrology (PNRH) (grant 62 no. 200).

REFERENCES

Belhadj N, Joannis C, Raimbault G. 1995. Modelling of rainfall induced infiltration into separate sewerage. *Water Sciences and Technology* **32**: 161–168.

Berthier E, Andrieu H, Rodriguez F. 1999. The Rezé urban catchment database. *Water Ressources Research* **35**: 1915–1919.

Berthier E, Andrieu H, Creutin JD. 2004. The role of soil in the generation of urban runoff: development and verification of a 2D model. *Journal of Hydrology* **299**: 252–266.

Boone A, Calvet JC, Noilhan J. 1999. Inclusion of a third soil layer in a land surface scheme using the force–restore method. *Journal of Applied Meteorology* **38**: 1611–1630.

Boyd MJ, Buffil MC, Knee RM. 1993. Pervious and impervious runoff in urban catchments. *Hydrological Sciences* **38**: 463–478.

Boyd MJ, Buffil MC, Knee RM. 1994. Predicting pervious and impervious storm runoff from urban drainage basins. *Hydrological Sciences* **39**: 321–332.

Cooley LA, Brown JER, Maghsoodloo S. 2001. Developing critical field permeability and pavement density values for coarse-graded superpave pavements. *Transportation Research Record* **1761**: 41–49.

Deardorff JW. 1977. A parameterization of ground surface moisture content for use in atmospheric prediction models. *Journal of Applied Meteorology* **16**: 1182–1185.

Dumenil H, Todini E. 1992. A rainfall–runoff scheme for use in the Hamburg climate model. *Climate Dynamics* **12**: 21–35.

Dupasquier B, Joannis C, Raimbault G, Zimmer D. 1998. Two types of models for investigating infiltration into separate sewerage. In *Conference on Application of Models in Water Management, Aquatech'98*, Amsterdam, Netherlands; 34–41.

Dupont S. 2001. *Modélisation dynamique et thermodynamique de la canopée urbaine: réalisation du modèle de sols urbains pour SUBMESO*. PhD thesis, Université de Paris Sorbonne, France.

Grimmond CSB, Oke TR. 1991. An evapotranspiration-interception model for urban areas. *Water Ressources Research* **27**: 1739–1755.

Grimmond CSB, Oke TR. 1999a. Evapotranspiration rates in urban areas. In *Impacts of Urban Growth on Surface Water and Groundwater Quality*, Reichard EG, Hauchman FS, Sancha AM (eds). IAHS Publication No. 259. IAHS Press: Wallingford; 235–243.

Grimmond CSB, Oke TR. 1999b. Aerodynamic properties of urban areas derived from analysis of surface form. *Journal of Applied Meteorology* **38**: 1262–1292.

Grimmond CSB, Oke TR, Steyn DG. 1986. Urban water balance. 1. A model for daily totals. *Water Ressources Research* **22**: 1397–1403.

Habets F, Etchevers R, Golaz C, Leblois E, Ledoux E, Martin E, Noilhan J, Ottlé C. 1999. Simulation of the water budget and the river flows of the Rhône basin. *Journal of Geophysical Research* **104**: 31145–31172.

Hassan HF, White TD. 1997. Laboratory and field moisture conditions for flexible pavement. *Transportation Research Record* **1568**: 96–105.

Hollis GE, Ovenden JC. 1988a. The quantity of stormwater runoff from ten stretches of road, a car park and eight roofs in Hertfordshire, England during 1983. *Hydrological Processes* **2**: 227–243.

Hollis GE, Ovenden JC. 1988b. One year irrigation experiment to assess losses and runoff volume relationships for a residential road in Hertfordshire, England. *Hydrological Processes* **2**: 61–74.

Lemonsu A, Grimmond CSB, Masson V. 2004. Modelisation of the surface energy budget of an old Mediterranean city core. *Journal of Applied Meteorology* **43**: 312–327.

Masson V. 2000. A physically-based scheme for the urban energy budget in atmospheric models. *Boundary-Layer Meteorology* **94**: 357–397.

Masson V, Grimmond CSB, Oke TR. 2002. Evaluation of the town energy balance (TEB) scheme with direct measurements from dry districts in two cities. *Journal of Applied Meteorology* **41**: 1011–1026.

Mills GM. 1993. Simulation of the energy budget of an urban canyon—I: model structure and sensitivity test. *Atmospheric Environment, Part B: Urban Atmosphere* **27**: 157–170.

Nash JE, Sutcliffe JV. 1970. River flow forecasting through conceptual models. 1.A: Discussion of principles. *Journal of Hydrology* **10**: 282–290.

Noilhan J, Mahfouf JF. 1996. The ISBA land surface parameterization scheme. *Global Planetary Change* **13**: 145–159.

Noilhan J, Planton S. 1989. A simple parameterization of land surface processes for meteorological models. *Monthly Weather Review* **117**: 536–549.

Oke TR. 1982. The energic basis of the urban heat island. *Quarterly Journal of the Royal Meteorological Society* **108**: 1–24.

Oke TR. 1987. *Boundary Layer Climates*, 2nd edition. Methuen: London.

Prata AJ. 1996. A new long-wave formula for estimating downward clear-sky radiation at the surface. *Quarterly Journal of the Royal Meteorological Society* **122**: 1127–1151.

Ragab R, Bromley J, Cooper JD, Gash JHC. 2003a. Experimental study of water fluxes in a residential area. 1. Rainfall, roof runoff and evaporation: the effect of slope and aspect. *Hydrological Processes* **17**: 2409–2422.

Ragab R, Rosier P, Dixon A, Bromley J, Cooper JD. 2003b. Experimental study of water fluxes in a residential area. 2. Road infiltration, runoff and evaporation. *Hydrological Processes* **17**: 2423–2437.

Ramier D, Berthier E, Andrieu H. 2004. An urban lysimeter to assess runoff losses on asphalt concrete plates. *Physics and Chemistry of the Earth* **29**: 839–847.

Rodriguez F, Andrieu H, Zech Y. 2000. Evaluation of a distributed model for urban catchments using a 7-year continuous data series. *Hydrological Processes* **14**: 899–914.

DOI: 10.1002/hyp